Anisotropic Internal Stress in Landfast Ice from Canadian Arctic Archipelago

Yukie Hata, Bruno Tremblay
Atmospheric and Oceanic Sciences, McGill University, Montreal, QC, Canada

1. Introduction and Description

A better understanding of landfast ice is indispensable to improve the simulation of high latitude climate since landfast ice covers 1.8×10^6 km^2 ($\sim$ 20 %) of the Arctic Ocean and its average annual duration is over seven months. An internal Ice Stress Buoy (ISB) was deployed near the center of a multiyear floe in the Viscount Melville Sound in the Canadian Arctic Archipelago (CAA). The buoy collected hourly internal sea-ice stress, GPS coordinates, air temperature and orientation between October 10, 2010 and August 17, 2011, which include irresponsible stress data from June 19 - August 17, 2011.

2. Ice Motion and Landfast Season

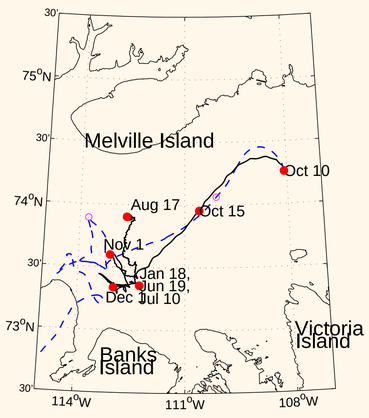

Figure: The drift of the multiyear ice floe from October 10, 2010 to August 17, 2011.

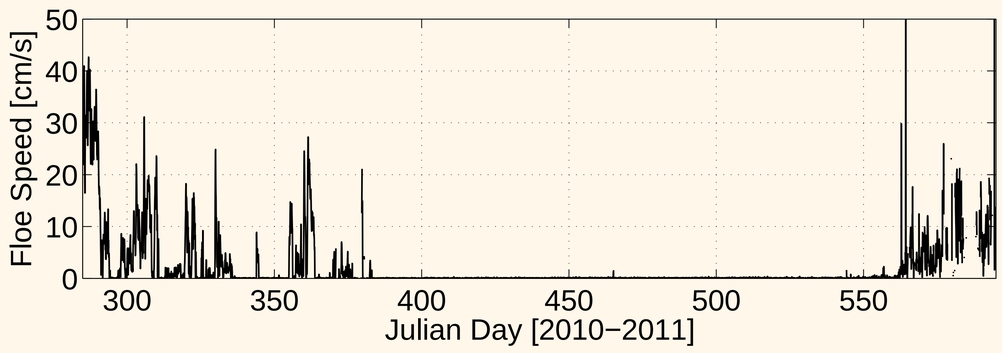

Figure: The time series of speed of the multiyear ice drift from October 10, 2010 to August 17, 2011.

The ISB was deployed on October 10, 2010 (Julian Day 283) at 7415′ North, 10805′ West in the Viscount Melville Sound within the CAA. From January 18 (JD 383) to July 10 (JD 556) the ice was landfast.

3. Firstyear Sea-Ice Strength Estimates

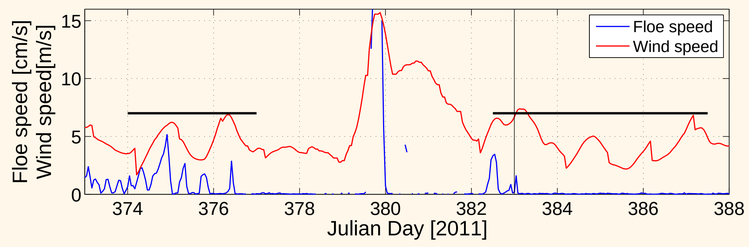

Figure: Time series of floe speed (in blue) and GEM reanalysis wind data [5] (in red) before and after sea ice became landfast on January 18 (JD 383)

- Integrating the wind force acting on ice floe by [2] :

$$\tau_a \times L \tag{1}$$

where τ_a ($= C_{da}\rho_a|\mathbf{u_a}|^2$) is surface wind force, and L (170 km) is the full width of the Parry Channel

- Estimate firstyear ice strength is around 30 kN/m.

4. Internal Ice Stresses

Principal Stresses and Air Temperature

Both σ_1 and σ_2 has high correlation with temperature (r^2 = 0.81 and 0.67, respectively).

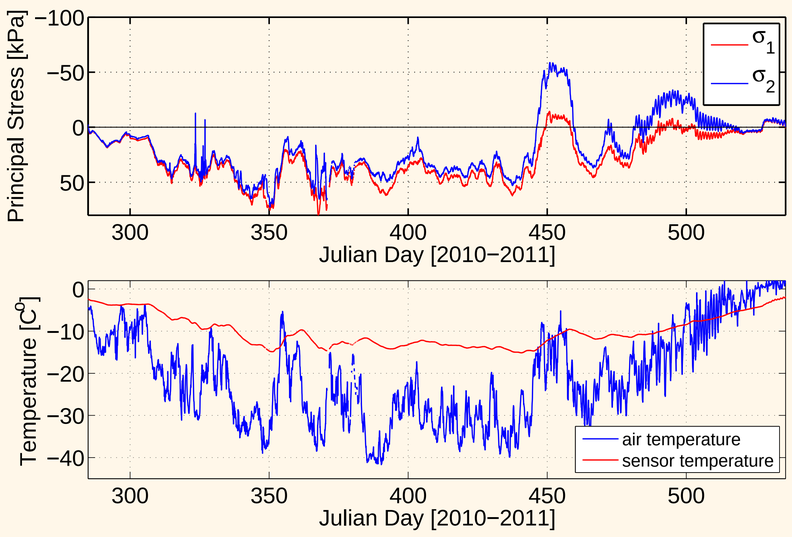

Figure: The time series of (top) principal stresses (σ_1 and σ_2) and (bottom) air and sensor temperatures between October 10, 2010 to June 17, 2011. Note that principal stresses are plotted negative upward to see clearer correlation with surface air temperature.

Sudden Short-Lived Peaks in Stresses

The internal sea-ice stress data shows high frequency fluctuations on November 19 - 23 (JD 323 - 327), December 4 - 5 (JD 338 - 339), December 14 - 15 (JD 348 - 349) and on January 2 - 6 (JD 366 - 371) when the floe speed drops to zero momentarily We interpret these sudden short-lived peaks in stresses accompanied by floe stoppage as collisions between multiyear ice floes.

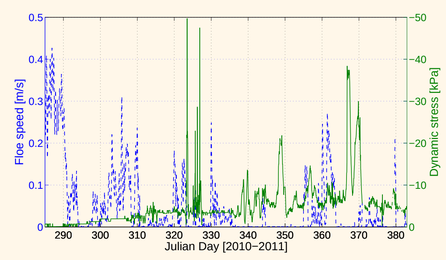

Figure: Time series of floe speed (in blue) and stress data (σ_2 - σ_1: in green).

$\sigma_2 - \sigma_1$ and wind speed

$\sigma_2 - \sigma_1$ is often interpreted as dynamic stresses [1], however, $\sigma_2 - \sigma_1$ has very low correlation with wind speed (r^2 = 0.13) in CAA. We interpret this result as an indication of the presence of anisotropy in coastal sea ice of the CAA by the preferred c-axis alignment [4].

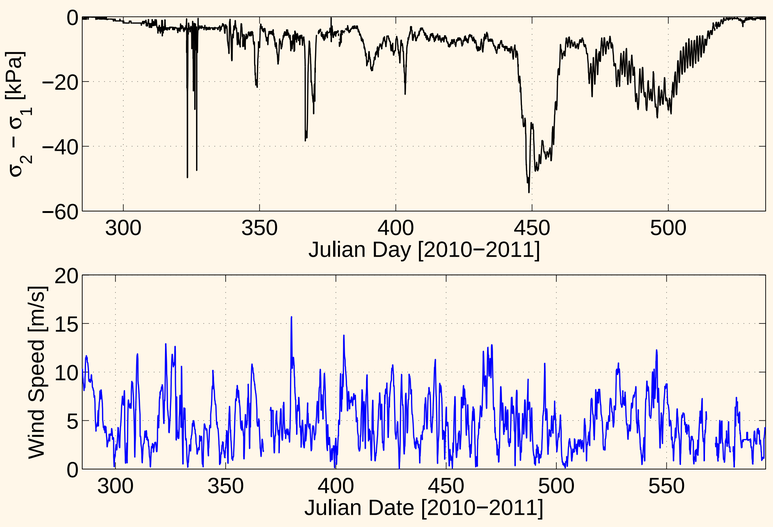

Figure: The time series of (top) σ_2 - σ_1 and (bottom) wind speed around the floe [5].

5. Anisotropic Thermal Stress Model

Model Equations 1: A 1.5D anisotropic thermal stress model based on linear elasticity theory

$$\sigma_{11}^{th}(z) = \frac{E_1}{1-\nu_1\nu_2}\left(\left[\frac{\int_{-h}^{0} E_1\alpha\Delta\theta_{(z)}dz}{\int_{-h}^{0} E_1 dz} - \alpha\Delta\theta_{(z)}\right] + \nu_2\left[\frac{\int_{-h}^{0} E_2\alpha\Delta\theta_{(z)}dz}{\int_{-h}^{0} E_2 dz} - \alpha\Delta\theta_{(z)}\right]\right)$$

$$\sigma_{22}^{th}(z) = \frac{E_2}{1-\nu_1\nu_2}\left(\left[\frac{\int_{-h}^{0} E_2\alpha\Delta\theta_{(z)}dz}{\int_{-h}^{0} E_2 dz} - \alpha\Delta\theta_{(z)}\right] + \nu_1\left[\frac{\int_{-h}^{0} E_1\alpha\Delta\theta_{(z)}dz}{\int_{-h}^{0} E_1 dz} - \alpha\Delta\theta_{(z)}\right]\right)$$

where internal ice temperature is calculated by the 1D thermodynamic model of [3].

- Youngs modulus, E_1 = 0.2 GPa (parallel to c-axis) and E_2 = 0.14 GPa (normal to c-axis) are required.
- The simulation is in some agreement with observed stress data.
- The principal stresses switch order when large surface warming and cooling are present.
- The deviation between the measured and simulated stress grows as the surface temperature gets colder. → due to stress relaxation via viscous creep.

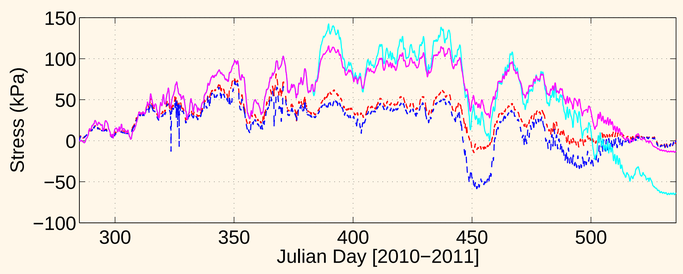

Figure: Time series of observed principal stresses and simulated internal sea ice thermal stresses at the depth of the sensor. No snow cover and no stress relaxation are assumed in the simulation.

Model Equations 2: Adding a simple relaxation term

$$\frac{\partial\sigma^{tot}}{\partial t} = \frac{\partial\sigma^{th}}{\partial t} - \frac{1}{r}(\sigma^{tot} - \sigma_0)$$

- The relaxation time constant = 110 days is required.
- The simulation is in better agreement with observed stress data.
- The stress relaxation via viscous creep present. → The compressive stress would present at the beginning of the melt season instead of zero stress.

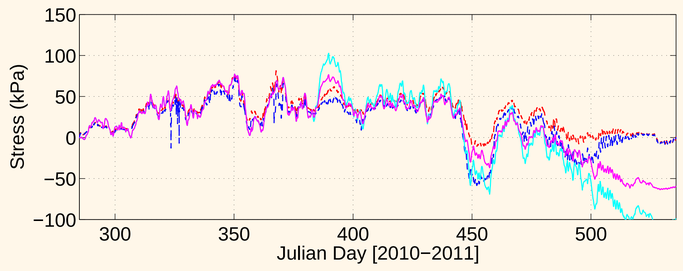

Figure: Time series of observed principal stresses and simulated internal sea ice thermal stresses at the depth of the sensor. No snow cover and stress relaxation via viscous creep with a relaxation time scale of 110 days (2640 hours) are assumed in the simulation.

Best Match

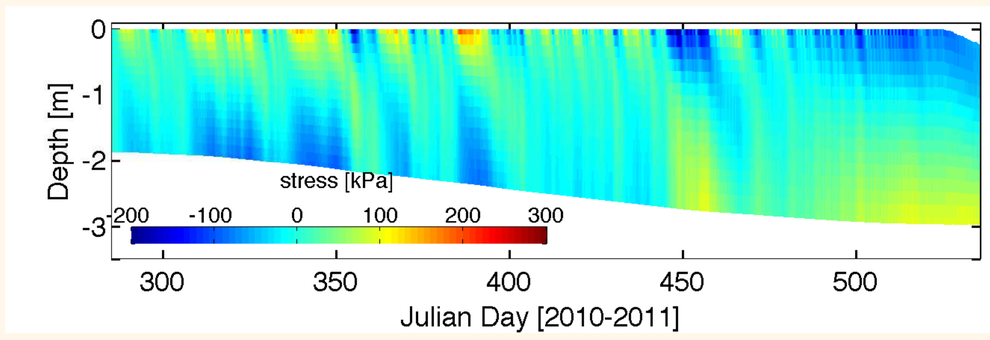

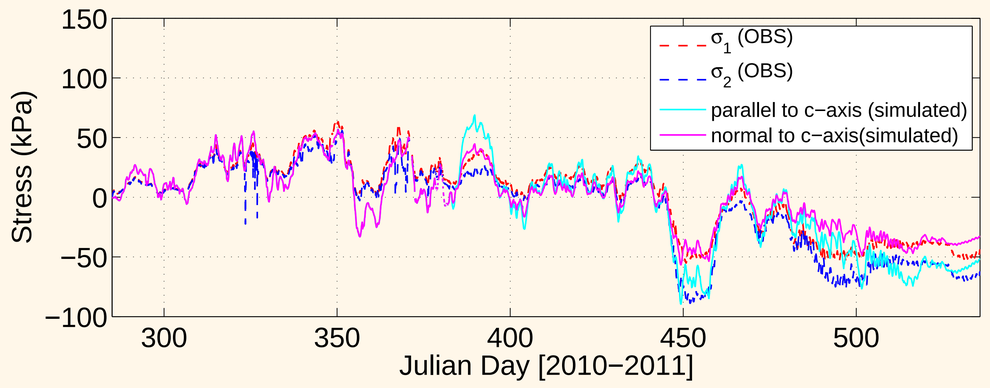

Figure: The time series of (top) stress vertical distribution and (bottom) stress at the sensor depth.

- The simulation is in good agreement with observed stress data.
- The relaxation time constant decreases to 720 hours.
- Compressive stress at the beginning of melt season is assumed. -30 kPa in σ_1 and -50 kPa in σ_2 are required for best match.
- The vertical distribution of the thermal stress from the simulation shows that when tensile stresses develop near ice surface, compressive stresses develop near the bottom of the ice.

6. Conclusion

- Landfast season in the Viscount Melville Sound last nearly six months from January 18 to July 10, 2011.
- A few events when dynamic stresses are large associating with floe-floe collision.
- A compressive strength of firstyear sea ice of 30 kN/m is estimated
- The observed stress data is highly correlate with changes in surface air temperature and not significantly correlated with the magnitude of the wind speed.
- Anisotropy in sea ice is responsible for the difference in principal stresses as opposed to dynamic stresses in region where sea ice is isotropic [e.g.][]Richter-Menge2002, Hutchings2010.
- A 1.5D anisotropic thermal stress model for sea ice including the effect of stress relaxation via viscous creep results in a good agreement with the observed principal stresses, when stress relaxation via viscous creep is considered.

7. References

Richter-Menge, J. A. and Elder, B. C., 1998:Characteristics of pack ice stress in the Alaskan Beaufort Sea, *Journal of Geophysical Research.*, **103,** 817–829

Tremblay, L.-B., and M.Hakakian, 2006: Estimating the sea ice compressive strength from satellite-derived sea ice drift and NCEP reanalysis Data, *Journal of physical oceanography.*, **36,** 2165-2172

Huwald, H. and Tremblay, L. B. and Blatter, H, 2005: A multilayer sigma-coordinate thermodynamic sea ice model: Validation against Surface Heat Budget of the Arctic Ocean (SHEBA)/Sea Ice Model Intercomparison Project Part 2 (SIMIP2) data, *Journal of Geophysical Research.*, **110,** C05010

Weeks, W. F. and Gow, A. J., 2007: Preferred crystal orientations in the fast ice along the margins of the Arctic Ocean , *Journal of Geophysical Research*, **83,** 5105

Surface wind data from GEM high resolution model, Environmental Canada (G. Smith).

yukie.hata@mail.mcgill.ca